THE GUARDIAN PROJECT: REASONS, CONCEPT AND ADVANTAGES OF A NOVEL OBSTACLE PROXIMITY LIDAR SYSTEM

Session Subject: Aircraft Systems & Avionics

Massimo Brunetti, **massimo.brunetti@agustawestland.com**

R&T Project Leader at AgustaWestland S.p.a.

Cascina Costa, I-21017 Samarate-Varese, ITALY

ABSTRACT

Helicopters are used all over the world for missions where “hovering” is the only feasible option. Among these, Emergency Medical Service and Search And Rescue stand out for the noble aim and the evident risk. This paper takes you to the realm of the EMS/SAR operations and goes through the AW Guardian Project, launched in 2009 to tackle helicopter accidents in confined space. System requirements are captured and a preliminary design is put forward, based on Light Detection and Ranging sensors. The paper explains how LIDAR sensors work and how they can benefit helicopter safety. LIDAR raw data are manipulated into a more intelligible form and system HMI is tailored on a reference cockpit. The system architecture is completed with ancillary LRUs and the system installation adapted to the AW139. Design proposal is then verified and validated through a series of ground tests, simulations and flight trials which enabled transition from TRL0 to TRL6 and even further, to system certification achieved in 2014 with EASA. The system is now a proprietary solution of AgustaWestland, a registered logo and an optional kit available on the AW139 helicopter under the name of OPLS™. When equipped with the OPLS™, pilots can rely on an invisible “eye” monitoring with superior accuracy the obstacles in plane with the main rotor disc, by day, by night, over 360°.

ACRONYMS

AFCS	Automatic Flight Control System
API	Application Programme Interface
ATP	Acceptance Test Procedure
AW	AgustaWestland
BERP	British Experimental Rotor Programme
COTS	Commercial Off The Shelf
CPLT	Co-pilot
DAL	Design Assurance Level
DOC	Direct Operational Costs
DVI	Digital Video Interface
EASA	European Aviation Safety Agency
EMS	Emergency Medical Service
EHST	European Helicopter Safety Team
EPGD	Electrical Power Generation Distribution
FAA	Federal Aviation Administration
FOV	Field Of View
GPS	Global Positioning System
GUI	Graphic Use Interface
HMI	Human Machine Interface
HRTF	Head Related Transfer Function
ICS	Inter Communication System
IIR	Infinite Impulse Response
JAR	Joint Aviation Requirements
LAN	Local Area Network
LCD	Liquid Crystal Display
LIDAR	Light Detection And Ranging
LRU	Line Replaceable Unit
MFD	Multi Function Display
NASA	National Aeronautics Space Administration
NTSB	National Transportation Safety Board
NVG	Night Vision Goggles
OPLS	Obstacle Proximity LIDAR System
PFD	Primary Flight Display
PLT	Pilot
R&T	Research & Technology
SAR	Search And Rescue
SNR	Signal to Noise Ratio
SVGA	Super Video Graphics Array
TAWS	Terrain Awareness Warning System
TRL	Technology Readiness Level
VNV	Verification and Validation
VTOL	Vertical Take-Off Landing

1. REASONS

Emergency medical service is one of the most popular helicopter applications and definitely, one of the riskiest. The inherent instability of helicopters, the high workload environment and the often unplanned nature of the flight route and landing zone, all contribute to the unique nature of these missions.

Accident statistics don't lie.

In USA, according to NTSB, 2008 was especially grim with 13 helicopter ambulance crashes and 29 deaths [Reference 1]. The situation has escalated to public crisis level with the increased number of private operators and aircraft. In 1980 there were 50 EMS helicopters, in 1990 almost 300 and in 2008 as many as 668 [Reference 2]. More than half of EMS helicopter crashes happen at night or in poor visibility, and nearly half of all fatal crashes occur at accident scene where terrain can pose risks. On the other hand, "*medical service reimbursements depend solely on flown distance so that there is no business incentive for flying twin-engine helicopters, or installing anything beyond the minimum safety equipment. The decision of safety equipment or to install safety equipment is left up to the operator*" [Reference 3].

In Europe, according to EHST, 2008 was equally a bad year with 15 helicopters accidents and 6 fatalities recorded during Commercial Air Transportation and Aerial Work operations [Reference 4]. Using a helicopter for these purposes can result in pushing the helicopter and pilot towards the limits of their capabilities and operation close to terrain or obstacles, a situation very common both to EMS and SAR. Getting to figures and tables, the most common standard problem involved in fatal accidents was pilot judgment & actions followed by pilot's situation awareness (Figure 2). These were recognized in 35% of the analyzed accidents and traced back to inadequate considerations of obstacles, reduced visibility, aircraft position and hazards, diverted attention and low flight near wires.

Figure 1 – EMS/SAR operation on Italian Alps

Actually, the assistance to operations in confined space is both a civil and military need. For instance, combat SAR helicopters have benefited through the years of self-sealing tanks, shielded fuselages and bullet-proof controls but main and tail rotor blades are still vulnerable. According to a NASA survey, of all helicopter accidents occurred in USA over the last thirty years and due to obstacle collision, 42% originated from tail rotor strike and 34% from main rotor [Reference 5]. This issue was at the heart of the BERP IV programme and influenced the design of the new rotor blade generation for the AW101 helicopter: *"The need for enhanced resistance to impact damage was a unanimous conclusion from all three services consulted"* [Reference 6]. In a similar manner, fan-in-fin represents an improvement over the open tail rotor architecture which however does not completely eliminate the risk of items ingestion and structural damage.

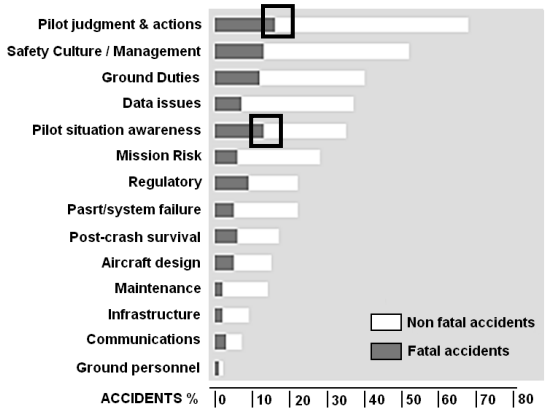

Figure 2– EHST accidents analysis (2005-2008)

To aid helicopter operations in confined spaces, avoid obstacle collisions and ease the approach to unprepared rescue sites, AgustaWestland decided to invest in 2009 in the development of a novel Obstacle Proximity LIDAR System. The project was given the name of Guardian (from the intent to guard the helicopter safety) and led to a certified product five years later. The chapters that follow describe the activities and results which enabled transition from TRL0 (*basic principles observed and reported*) to TRL6 (*system demonstration in aerospace environment*).

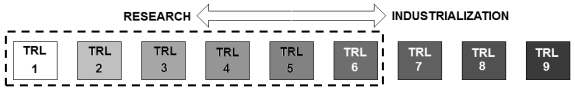

Figure 3 – Technology Readiness Level

2. CONCEPT

The birth of a new avionic system is never easy, sometimes encouraged by the market, often frowned upon by authorities, always the result of countless verifications and validations. From this perspective, the Guardian project and the commercial product that developed was not an exception. This chapter exemplifies the iterative process that starting from initial system requirements progressed to the final system design through ground tests, laboratory simulations and flight trials. The whole process can be also interpreted as a problem of design optimization in the space of the system requirements (Figure 4). Optimum design D° is considered made up of several normalized aspects (1). Each aspect is then projected on requirements axes to establish a link in the form of projection coefficients (directional cosines d_i).

(1) $\vec{D}^{\circ} = \sum_K \vec{D}^{\circ K} = \sum_K \sum_1^N D^{\circ K}_i \cdot \hat{r}_i = \sum_K \sum_1^N d_i^K \cdot \hat{r}_i$

In a similar manner, design proposal D is projected and modulated by VNV coefficients ($w_i \leq 1$) expressing the system effectiveness in connection with the system requirements (2).

(2) $\vec{D} = \sum_K \vec{D}^K = \sum_K \sum_1^N D_i^K \cdot \hat{r}_i = \sum_K \sum_1^N d_i^K w_i^K \cdot \hat{r}_i$

Design vector has thus a magnitude which is a monotone function of the VNV coefficients and a figure of merit to be maximized.

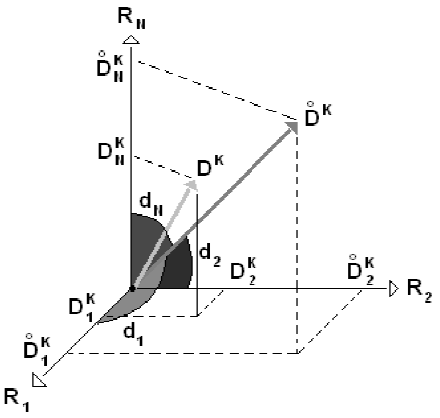

Figure 4 – Design vs. Requirements

2.1 System Requirements

System requirements were captured in cooperation with company test pilots and the operators who provide SAR/EMS service in the north part of Italy. Here follow the most significant.

R_1 *Enhance the situational awareness*. Pilots suggested to developing a system that enhanced human sight without upsetting traditional see & avoiding techniques. Autopilot coupling was judged attractive but not immediately achievable for the significant effort associated to adequate hardware and software DAL.

R_2 *Ease the approach.* Operators confirmed to hover nearby obstacles for extended periods of time whilst traditional obstacle avoidance systems (like TAWS) are targeted to long range collisions which are averted by aggressive alarms, generated with sufficient notice. Pilots suggested focusing on a short range (up to 10m), accurate (~0.5m) distance measurement system.

R_3 *Reduce the workload.* Pilots recommended to develop a simple and intuitive interface, with a minimum number of controls and indicators which did not duplicate but rather integrate what is already available in the cockpit.

R_4 *Avert rotor strike.* The consequences of a main rotor collision are often catastrophic but statistics indicate tail rotor as the most vulnerable part during low-speed, low-altitude operations. Operators asked for a system solution which protected both the main and the tail rotor.

R_5 *Simple & effective.* Operators suggested to develop a system with a low purchase price and DOC. Weight was considered a main driver for the selection of a suitable obstacle detector.

R_6 *Multi-platform.* Operators asked for a system compatible with the AW139 fleet and other helicopters (e.g. AW109). Pilots suggested developing a self-contained system.

R_7 *Be harmless.* Operators asked for a system that was harmless and compatible with landing and take-off from crowded areas. By certification paradigm, the system had not to interfere with the basic aircraft equipment.

R_8 *All weather proof.* Operators confirmed to fly mostly in good weather (visibility ≥ 2Km) but also that poor conditions couldn't be excluded. Pilots suggested developing an all-weather solution or one as insensitive as possible to adverse elements (i.e. rain and snow).

2.2 Design Proposal

The following design aspects originated from the careful consideration of the previous system requirements.

D^1 *Sensing Technology.* In order to detect obstacles, it was decided to look for active technology (i.e. not requiring a cooperative target), better if available as COTS. First option was ultrasound sensors, like those exploited by parking systems. These tiny sensors emit ultrasounds pulses (~100Khz) which combine excellent accuracy (~1cm) and weight (~0.01Kg) but are limited to a short range (~1m) and suffer from pressure fluctuations (like those induced by the rotor downwash). Second option was radar sensors like those exploited by aircraft altimeters. These sensors work on the basis of high frequency modulation (~10GHz) and feature high immunity to poor weather conditions. They also offer a fair accuracy (~1ft) over excellent range (~1000ft) but are not particularly light (~1Kg) nor steerable. Third option was laser sensors, like those exploited by industrial robots. These sensors emit quick pulses (~1ns) that allow for eye-safe, high SNR distance measurements based on time-of-flight (3).

$$(3)\quad d = c \cdot \Delta t / 2$$

They also offer good accuracy (~10cm) over a fair range (~10m) and they're compact enough (~0.1Kg) to be steered. When combined with a resolver, these sensors turn into multi-axes telemeters usually known as LIDAR (Figure 5).

$$(4)\quad \begin{bmatrix} d \\ \omega \end{bmatrix} = \begin{bmatrix} d_0 & \cdots & d_{FOV} \\ \omega_0 & \cdots & \omega_{FOV} \end{bmatrix}$$

LIDARs can map surfaces with high spatial and temporal resolution and can be exploited for obstacle detection, either on ground or in flight.

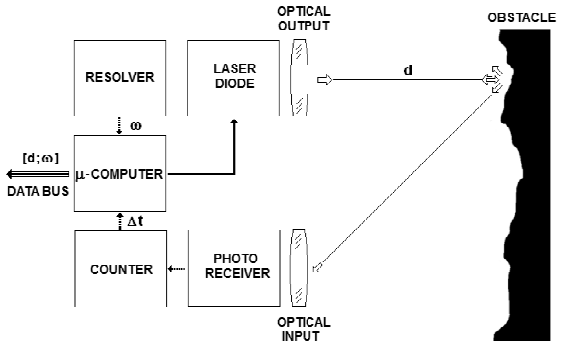

Figure 5- LIDAR principle of operation.

It was therefore decided to focus on LIDARs and to adopt a small, compact unit of 1.1Kg, featuring a laser class1 (eye-safe) and a planar FOV of 270°x50m in steps of 0.25°, with a refresh of 25Hz.

D^2 *Data processing.* In order to extend the FOV of the selected LIDAR unit it was figured out to install two (or more) of these onboard a helicopter and to map the output raw data (4) into a common reference, centred on the main rotor hub, by means of a simple rigid transformation (5).

$$(5)\quad \begin{bmatrix} X \\ Y \end{bmatrix} = \begin{bmatrix} A \\ B \end{bmatrix} + \begin{bmatrix} \cos\alpha & -\sin\alpha \\ \sin\alpha & \cos\alpha \end{bmatrix} \cdot \begin{bmatrix} x \\ y \end{bmatrix}$$

The blend of the individual contributions is thus an omnidirectional profile of the obstacle (6).

$$(6)\quad \begin{bmatrix} D \\ \Omega \end{bmatrix} = \begin{bmatrix} D_0 & \cdots & D_{360} \\ \Omega_0 & \cdots & \Omega_{360} \end{bmatrix}$$

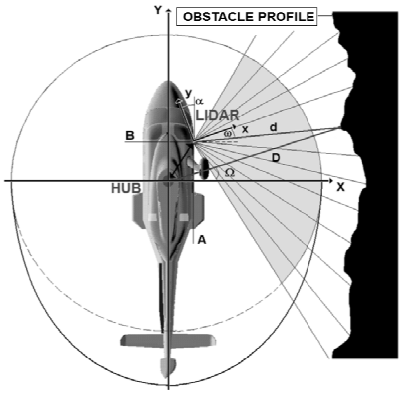

Figure 6 – Obstacle profile generation

On the other hand, rather than determining the position of each blade in the helicopter reference system, it was preferred to introduce a safety profile (7), inclusive of both the main and tail rotor footprint.

$$(7)\quad \begin{cases} X^2 + Y^2 = R_1^{\,2} \Leftrightarrow Y \geq 0 \\ \dfrac{X^2}{R_1^{\,2}} + \dfrac{Y^2}{R_2^{\,2}} = 1 \Leftrightarrow Y \leq 0 \end{cases}$$

This approach simplified the computation of the safety margin which immediately followed from comparison of the safety and the obstacle profiles.

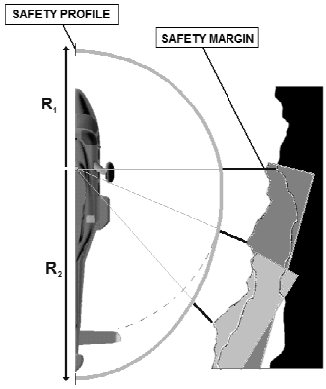

Figure 7 – Safety profile and safety margin

A set of digital filters was then implemented to reduce the impact of interferences on raw data.

This set included: range filter (to discard points within the helicopter safety profile), null filter (aimed at recovering missing samples or disrupted profiles), particle filter (to remove isolated, non persistant samples) and low pass filter (to smooth temporal fluctuations).

D[3] *Human machine interface.* The routines generating the video and audio indications were written in C++ with the help of an OpenGL® API. Resolution was set to 800x600 and layout was designed to match 3:4 display format (16:9 with black stripes). The final result is shown below (Figure 8) and included: the obstacle profile, the helicopter profile, the safety margin indication and a tracking beam steering to closest obstacle point. All these elements were superimposed on a homothetic 360°x25m FOV with polar grid, range captions and standard colours to prompt the recognition of the safety condition.

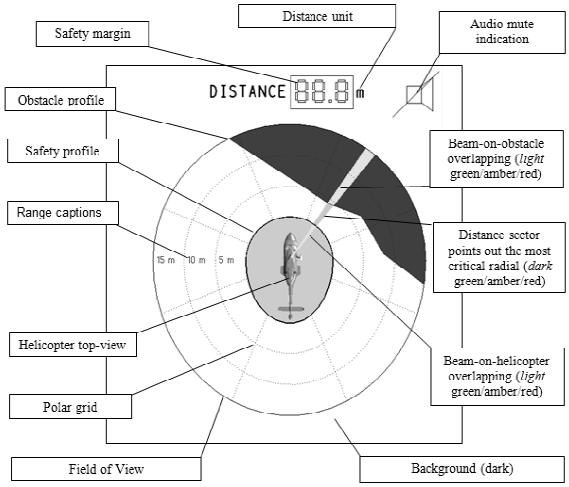

Figure 8 – Video HMI

Safety condition determination proceeded from comparison of the safety margin with two distance thresholds (warning and caution). These thresholds were left reconfigurable (to fulfil different customers' needs) and used to trigger a set of vocal announcements (upon band transition). A variable frequency tone was also introduced in the central band to simplify the interpreaton of the safety margin. A mute functionality was implemented to exclude the tone but automatically reengage it in case of danger (e.g transition to warning band).

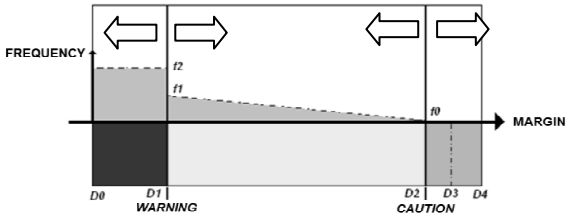

Figure 9 – Audio HMI

D[4] *System architecture.* Once the "eyes" of the Guardian were selected, a "brain" was needed. Therefore, a central computer unit was added to process LIDAR raw data and generate the video and audio indications in the cockpit (Figure 10). This latter was assumed to include one (or more) MFD, a monophonic ICS and provision for a dedicated control panel. A central computer unit was configured with a standard power supply board (28VDC), three Ethernet ports, a dual SVGA/DVI interface, a stereo output and two RS232/422 serial ports. One of these was exploited to connect the control panel while the other was reserved for optional system integration (e.g. 3D-Audio).

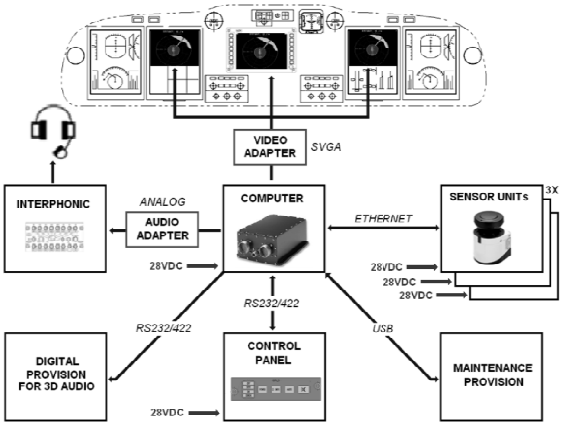

Figure 10 – System architecture

In order to curb costs and time, both the sensors and central computer unit were picked up from the COTS catalogue while the system control panel was developed on specification, for optimum harmonization with the rest of the cockpit. By specification, the control panel was set to operate at 28VDC, to accept a remote diming input, to be NVG compatible and to support few basic controls with feedback (power, mute, info). The feedback was enslaved to the computer status and the computer status was regulated by a finite state machine diagram. This solution proved consistent with the network "star" topology and prevented conflicts between the LRUs.

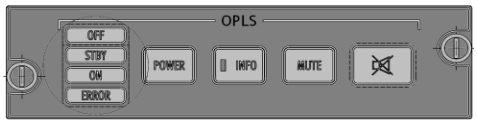

Figure 11 – System control panel

D[5] *System installation*. In order to achieve a complete coverage of the obstacles around the aircraft, it was decided to install three LIDAR units in the upper deck, as close as possible to the main rotor hub (Figure 12).

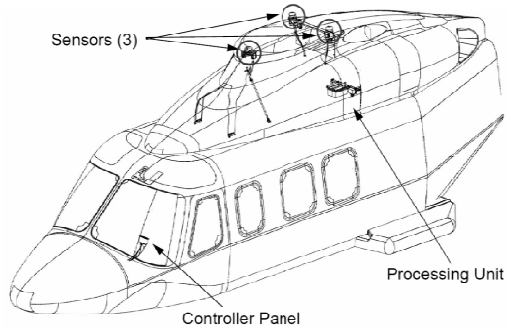

Figure 12 – LIDARs position

This solution ensured a wide scanning overlap, the tail rotor protection, the minimization of the optical interferences with the fuselage and a reduced projection error.

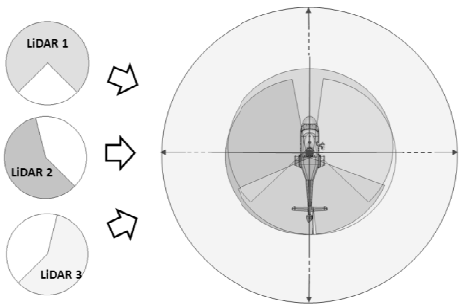

Figure 13 – LIDARs overlapping

Projection error (9) depends on a multitude of factors (like blade flapping, main rotor cone and obstacle slope) which cannot be totally compensated but usually result in a positive (conservative) margin.

(9) $PE = \Delta + \delta$

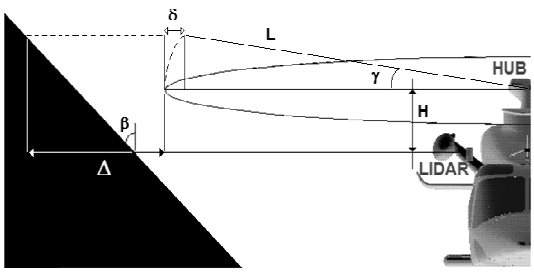

Figure 14 – Projection error

On the other hand, this solution raised some doubts in connection to the risk of sensor detachment or disallignment. As shown later in the paper, the former was mitigated by tests directed at assessing the robustness of the structural provision while the latter was managed by recourse to adjustable supports and a dedicated, calibration procedure.

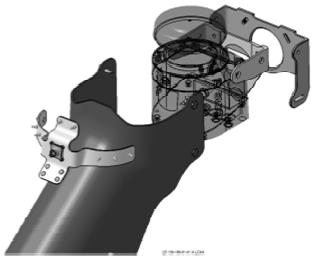

Figure 15 – forward LIDAR support

An excerpt of the calibration procedure is reported below (Figure 16) to outline the determination of azimuth error by triangulation, on the basis of acquired distances and angles.

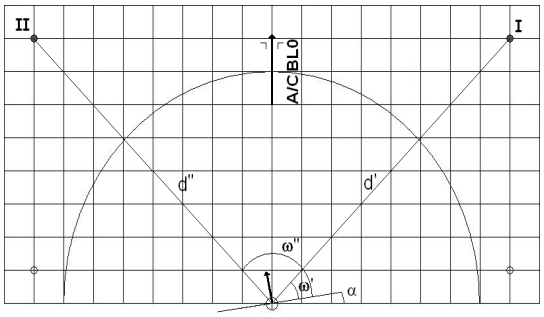

Figure 16 – Azimuth error triangulation

2.3 Verification And Validation

Scope of the verification is to ensure the compliance of the implemented design to specifications while scope of the validation is to assess the effectiveness of the system design implemented for the reference scenario. This chapter provides examples of both activities, from TRL0 to TRL6.

2.3.1 Technology assessment. This activity validated the use of the selected LIDAR unit and digital filters to detect obstacles of different shape, size and reflectivity. All the tests were carried using original setups on prepared sites.

a. Single LIDAR, ground-test. During this test, the selected LIDAR unit was installed on a moving cart, connected to a helicopter 28VDC battery and interfaced to a laptop via LAN (Figure 17). In order to minimize the source of uncertainty, all the data were recorded using the standard LIDAR GUI and post-processed by MATLAB®.

Figure 17 – Ground setup

Obstacles such as wooden and plastic pallets, painted in different colors to vary reflectivity, were illuminated at different distances and along different axes to assess the detection performance of the unit under test (Figure 18).

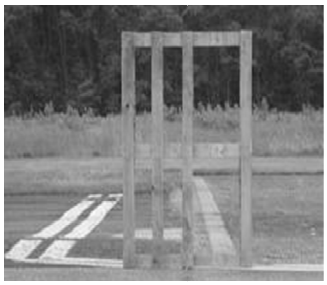

Figure 18 – Illuminated target

Linear error, angular resolution, cross-talk and sensitivity were verified to be in compliance with the official datasheet and well suited for the reference scenario.

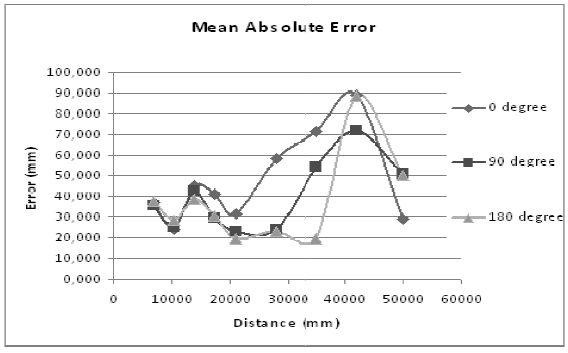

Figure 19 – Static linear error

b. Single LIDAR, flight-test. During this test, the selected LIDAR unit and a portable laser scale were installed coaxially, in the cabin of a real helicopter (Figure 20). The laser scale was used as a zero reference order unit and fastened to a graduated disc, for accurate azimuth orientation. The LIDAR was connected to the helicopter EPGD system and interfaced to the usual laptop computer. The laptop computer was uploaded with a custom GUI, designed to record LIDAR raw data and to control the implemented digital filters.

Figure 20 – Flight setup

In the first part of the experiment, the pilot was asked to hover beside a flat hangar and to hold the aircraft heading while laser scale was operated at different angles (Figure 21). LIDAR and laser scale distances (10) were then normalized and compared by T-Test. This test confirmed the coherency of the two sources, with a confidence level of ~92%.

$$d' = d \cdot \left[1 + tg(\alpha) \cdot tg(\beta)\right] \cdot \cos\alpha \tag{10}$$

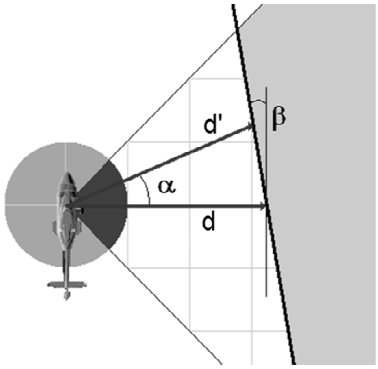

Figure 21 – Flight test procedure

In the second part of the experiment, the pilot performed a free flight around the hangar to test the effectiveness of the null and particle filters. The former successfully reconstructed the semi-transparent corner of the hangar while the latter eliminated all the false alarms triggered by the floating leaves.

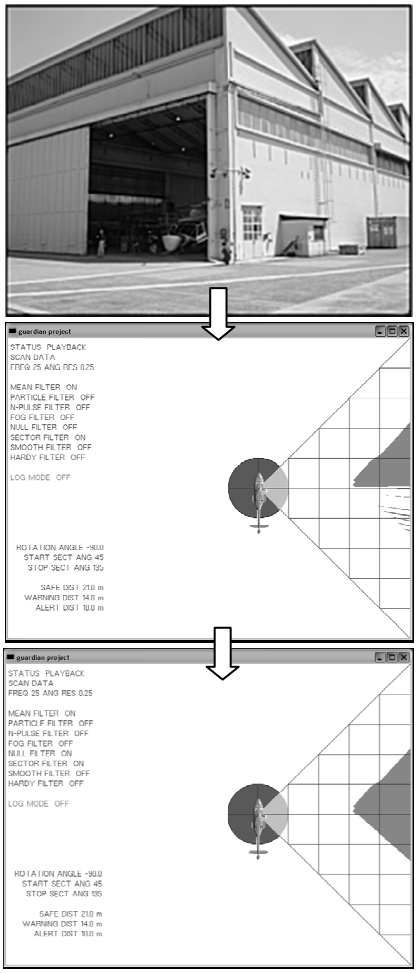

Figure 22 – Null filter test results

c. Multiple LIDAR, ground-test. During this test, three LIDAR units were mounted on a rigid bench, with adjustable forks and graduated discs (Figure 23).

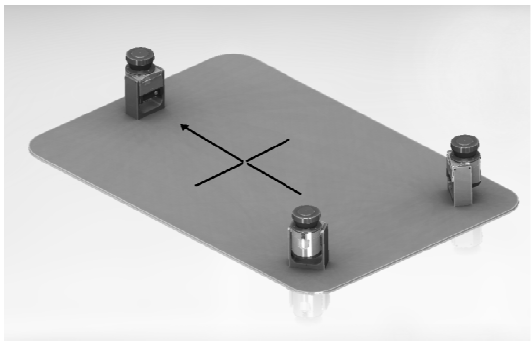

Figure 23 – Test bench

LIDARs were connected in parallel to a 28VDC power supply unit and multiplexed through an Ethernet switch into the usual laptop computer. The laptop computer was uploaded with a new GUI, including the rigid transformation (5) and complete video HMI. The bench was placed at the centre of a circular fence and a complex pattern made up of circular and radial indications was marked on ground, to reproduce a real scale version of the on screen layout (Figure 24). This pattern was then used to probe the system response at specific positions, with a target shaft of ~5cm width, over 360°.

Figure 24 – Test site

The three sensor configuration performed very well, detecting the shaft and the fence in the background at any angle with a linear (static) error of ~0.1m up to 25m. The merging algorithm was thus verified and the single LIDAR FOV successfully extended to 360° (Figure 25). This setup also allowed trimming the time constant of the low pass filter and to validate the azimuth calibration procedure. The former goal was achieved by pulling the shaft up and down and thus stimulating the system with an impulse signal. The latter was verified by rotating the LIDARs and computing the angle that by triangulation compensated the induced misalignment.

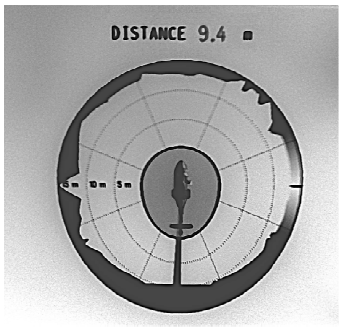

Figure 25 – Obstacle profile

2.3.2 HMI assessment. This activity validated the system HMI by means of real time, man in the loop simulations. Simulations were carried out with the help of professional SAR/EMS pilots, sitting on a mock-up, in a stereoscopic dome. The mock-up was representative of the AW169 helicopter cockpit and included: three large LCDs; a stereophonic headset; real control grips with force feedback (Figure 26). Both the cockpit and the dome were connected to a server running a modified version of the OPLS application. This latter was divided in four threads and the individual LIDAR data outputs were emulated consistently with the digital terrain database.

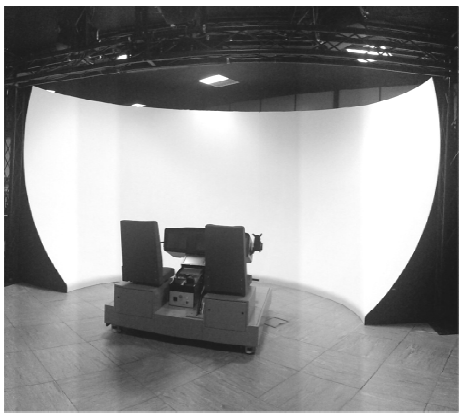

Figure 26 – HMI simulator

a. Heliport scenario. This scenario reproduced a runway bordered by hangars (Figure 27). The hangars were spaced widely, to validate the HMI under relatively simple conditions. System FOV was judged adequate for taxiing and for close distance operations while audio alarms were found to be affected by a little yet annoying delay. Delay time was reduced by compressing the audio tracks and optimizing the trigger routine.

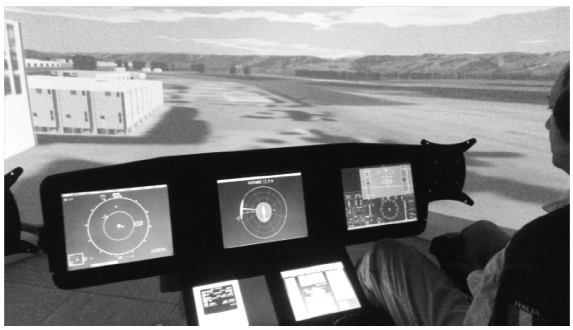

Figure 27 – Heliport scenario

b. Alpine scenario. This scenario simulated a SAR/EMS operation in the mountains. The synthetic environment consisted of concave and convex surfaces (a rocky cliff with ledges, bumps and vegetation), whose distance was pretty much difficult to estimate (Figure 28). The pilot was asked to approach the rescue site indicated by a smoke-producer, in the shortest time. Both the video and audio indications were judged helpful (especially the tracking beam) but pilots suggested modifying the mute functionality to make it available directly from the grips (i.e. without taking off the hands). This solution was transferred to production.

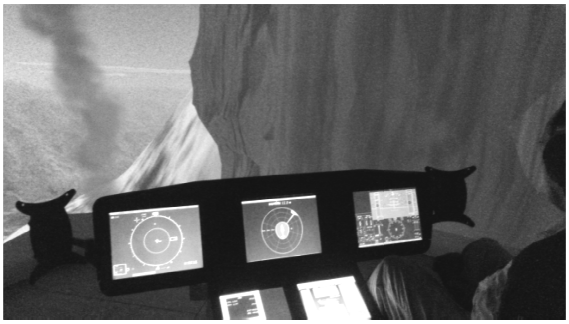

Figure 28 – Alpine scenario

2.3.3. System assessment. This activity validated the system architecture and installation onboard the AW139 helicopter. The AW139 was selected by virtue of its established SAR/EMS market and the advanced avionic provision which allowed for a seamless integration with the rest of the cockpit.

a. Helicopter ground-test. This activity was driven by a formal ATP directed at the verification of the LRUs physical installation and functional behaviour (Figure 29).

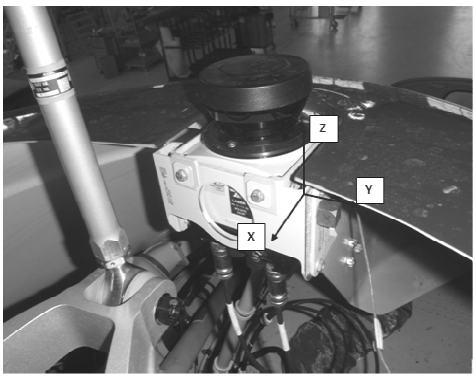

Figure 29 – Forward LIDAR installation

For instance, this procedure verified the absence of dangerous resonance (Figure 30) and the proper conductivity of the LIDAR supports as a lightning countermeasure.

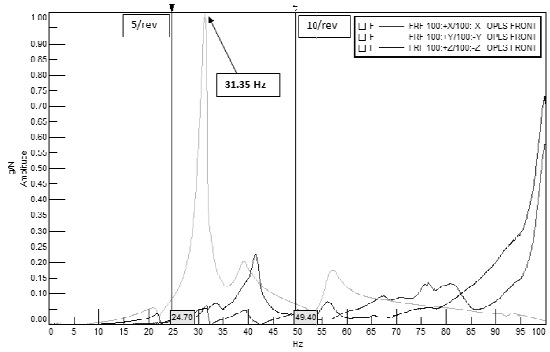

Figure 30 – Forward LIDAR rap-test

A functional check was then executed to verify the entire boot sequence, from initial power on to video formation on PLT and CPLT MFDs (Figure 31).

Figure 31 – System boot

Finally, the helicopter was towed outdoors, on a cleared site, and the system accuracy was assessed along concentric circles, with the aid of the usual target shaft (Figure 32). During the test, engines remained off while an external generator supplied the necessary electricity.

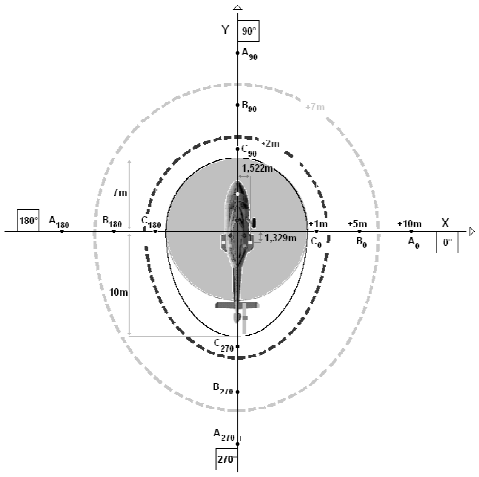

Figure 32 – Test pattern

The designed configuration consisting of three LIDAR sensors installed around the main rotor hub was able to detect the shaft at any point (even behind the tail) with a linear error of ~0.1m, up to 17m and a sensitivity of ~0.25° (Figure 33).

Figure 33 – Target shaft detection

b. Helicopter ground run. This activity was directed at the assessment of the HMI as per JAR-CS29 29.771 (PLT compartment), 29.773 (PLT view) and 29.777 (cockpit controls) certification requirements. This activity verified also the qualitative impact of the rotor downwash and the exhaust outflow on LIDARs. As such, the pilot was instructed to switch on the engines and perform taxiing along the company runway, nearby the adjacent hangars and vegetation. The same test was then repeated by night to validate the HMI and cockpit harmonization in low light conditions (Figure 34). Both sessions suggested to thicken the graphical layout and to raise the alarms volume but dispelled any doubt about the system installation.

Figure 34 – System integration (AW139)

c. Helicopter domestic flight. In this case, the pilot was instructed to hover nearby the company hangars, vegetation and scaffolds with the goal to validate the obstacle detection capability in a controlled environment. As such, test sites were prepared by ground personnel who assisted pilots at manoeuvring in the neighbourhood of specific markers. Markers were positioned at specific distance from the obstacles and watched through the aircraft chin bubble. At the end of the test, pilots confirmed that regardless of their grip and pedal inputs, system response remained always smooth and that numerical margin indication was very surprising because it was in apparent contrast with their first glance prediction. Also, the effectiveness of the digital filters was confirmed by the virtual absence of false alarms and the accurate level of the obstacle profile (Figure 35).

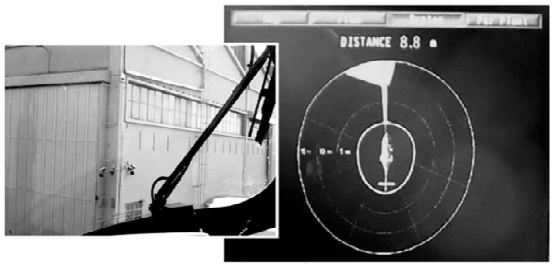

Figure 35 – Hangar detection

d. Helicopter outdoor flight. This was the last and most important test which validated the use of the system in the reference scenario. As such, the helicopter was refuelled, auxiliary cameras were taken on board and pilot headed for mountains, in search of a typical EMS/SAR rescue site (Figure 36).

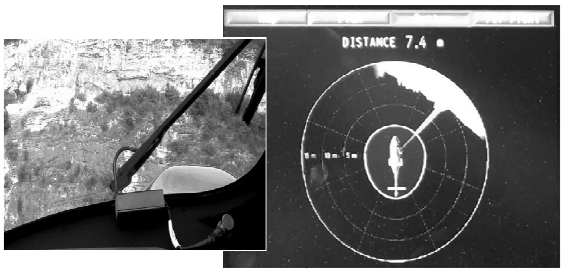

Figure 36 – Rocky cliff detection

Here, the pilot was instructed to perform a frontal approach, then to rotate the aircraft and

to expose the tail rotor to rocks and vegetation. The entire sequence was filmed and recorded several minutes of careful manoeuvring. Eventually, the obstacle profile entered the FOV and all the alarms were reproduced in the correct sequence, down to the warning band.

3. ADVANTAGES

Whilst the numerical distance information is not a useful indication per se, it is envisaged that by adequate training, EMS and SAR pilots will learn to interpret the system feedback and to associate it to the "real" safety condition. The advantages offered by the system are then evident considering that unlike human sight the system is able to detect obstacles as thin as few cm, 360° around the aircraft, up to 25m, both by day and by night, with a static accuracy of ~0.1m. Notably, test pilots agreed on the effectiveness of system indications and especially in conjunction with the hovering page, showing the ground speed vector on the PFD (Figure 37). The combination of these indications, generated by two independent systems working on the basis of different technologies (LIDAR and GPS) was enabled by the unique flexibility of the AW139 cockpit and well represented the "gap" filled out by the project.

Figure 37 – System in action (AW139)

The certification process which followed TRL6 extended the experimental test results and demonstrated compatibility of the system with the AW139 flight envelope. This allowed for the industrialization of the system which is now a proprietary solution of AgustaWestland and an optional kit available on the AW139 under the name of OPLS™. Although developed to assist EMS/SAR operators in hovering in confined space, it is the author's hope that the OPLS™ will spread over the entire AW family product and benefit a number of similar scenarios like taxing in congested heliports, aerial work operations on wind generators, departures from oilrigs or low speed approaches to skyscrapers (Figure 38).

Figure 38 – Urban scenario

The current version of the OPLS™ is definitely a step ahead towards safer SAR/EMS helicopter operations but still offers margins for improvement. Recalling the interpretation of the system design in the space of the system requirements (2), it is possible to identify the weakest design aspects (Figure 39) and outline the roadmap to the future system developments.

	R_1	R_2	R_3	R_4	R_5	R_6	R_7	R_8	$\lvert\cdot\rvert$
D^1	0.3	0	0	0.2	0.5	0.3	0.4	0.2	0.8
D^2	0.3	0.3	0.4	0.2	0.2	0	0	0.5	0.8
D^3	0.4	0.3	0.5	0.2	0.1	0.5	0	0.1	0.9
D^4	0	0.2	0	0.2	0.4	0.6	0	0.3	0.8
D^5	0.2	0.2	0	0.5	0.3	0.5	0.3	0.1	0.9
∑	1.1	1.0	0.8	1.4	1.5	1.8	.8	1.2	

$\lvert D\rvert$	3.5
$\lvert D°\rvert$	4.3

Figure 39 – Design evaluation

For instance, 3D-LIDAR technology may be used to extend the safety profile vertically, against obstacles from below or above the rotor disc while additional algorithms may be implemented to determine the aircraft trajectory and approaching speed. Finally, since head-down indications are impaired by the natural tendency to look out of the cockpit, 3D-Audio could be exploited to communicate the distance and direction to the nearest obstacle point (vector cue).

4. CONCLUSIONS

The Guardian project was launched in 2009 for the purpose of addressing the helicopter accidents that yearly occur during EMS/SAR operations in confined space. Preliminary investigations based on accident databases and customers' feedback, revealed an avionic gap to be filled out with a cost effective system, acting as a short range obstacle proximity sensor. The process that led from the initial system concept (TRL0) to a demonstration in the aerospace environment (TRL6) was schematized as a problem of design optimization and summarized in three steps:

- Requirements capture. This phase captured the functional, certification and economic requirements of the system, in order to outline the best direction to proceed.

- Design proposal. This phase addressed different design aspects like the sensing technology, algorithms, HMI, architecture and aircraft installation. Each aspect was discussed in connection with the system requirements to provide the best design proposal.
- Verification & validation. This phase assessed the compliance and effectiveness of the design proposal through ground tests, laboratory simulations and flight trials.

The positive results of the VNV phase and the seamless integration of the HMI on board the AW139 represented the premise for system certification, achieved in 2014 with EASA. The advantages of the system were finally exemplified and the contribution of emerging technologies considered in the scope of future developments.

ACKNOWLEDGMENTS

The author would like to acknowledge the support of Elilombarda and Airgreen in the capture and validation of system requirements, in particular Capt. C.Regis and Capt. I.Airaudi who encouraged the Guardian Programme. The successful programme is also a reflection of the efforts of the whole team within AgustaWestland whom thanks are extended.

REFERENCES

[1] C.Adams, "*EMS Hearing Spotlights and Safety Issues*", Rotor & Wing, March 2009

[2] S.Pope, "*Air Ambulance: A Closer Look*", Flying, July 2013

[3] C.Negroni, P.Veillette, "*Helicopter EMS Operations*", ISASI Forum, September 2010

[4] EHEST, "*Analysis of 2000-2005 European Helicopter Accidents*", Final Report, 2010

[5] FD.Harris, EF.Kasper, LE.Iseler, "*U.S. Civil Rotorcraft Accidents, 1963 through 1997*", NASA/TM-2000-209597, December 2000

[6] R.Harrison, S.Stacey, B.Hansford, "*BERP IV, The Design Development and Testing of an Advanced Rotor Blade*", AHS Annual Forum, April 2008

COPYRIGHT STATEMENT